Published in final edited form as:
J Proteome Res. 2014 February 7; 13(2): 681–691. doi:10.1021/pr4012393.

Glycomic Analysis of High Density Lipoprotein (HDL) Shows a Highly Sialylated Particle

Jincui Huang[1,3], **Hyeyoung Lee**[2,3], **Angela M. Zivkovic**[2,3], **Jennifer T. Smilowitz**[2,3], **Nancy Rivera**[2,3], **J. Bruce German**[2,3], and **Carlito B. Lebrilla**[1,3]

[1]Department of Chemistry, University of California, Davis, California 95616, United States.

[2]Department of Food Science and Technology, University of California, Davis, California 95616, United States

[3]Foods for Health Institute, University of California, Davis, California 95616, United States

Abstract

Many of the functional proteins and lipids in HDL particles are potentially glycosylated yet very little is known about the glycoconjugates of HDL. In this study, HDL was isolated from plasma by sequential micro-ultracentrifugation, followed by glycoprotein and glycolipid analysis. N-glycans, glycopeptides, and gangliosides were extracted and purified followed by analysis with nano-HPLC-Chip Q-TOF MS and MS/MS. HDL particles were found to be highly sialylated. Most of the N-glycans (~90%) from HDL glycoproteins were sialylated with one or two neuraminic acids (Neu5Ac). The most abundant N-glycan was a biantennary complex type glycan with two sialic acids ($Hexose_5HexNAc_4Neu5Ac_2$), and was found in multiple glycoproteins using site-specific glycosylation analysis. The observed O-glycans were all sialylated and most contained a core 1 structure with two Neu5Acs, including those that were associated with apolipoprotein CIII (ApoC-III) and fetuin A. GM3 (monosialoganglioside, NeuAc2-3Gal1-4Glc-Cer) and GD3 (disialoganglioside, NeuAc2-8NeuAc2-3Gal1-4Glc-Cer) were the major gangliosides in HDL. A 60% GM3 and 40% GD3 distribution was observed. Both GM3 and GD3 were composed of heterogeneous ceramide lipid tails, including d18:1/16:0 and d18:1/23:0. This report describes for the first time a glycomic approach for analyzing HDL, highlighting that HDL are highly sialylated particles.

Keywords

HDL; glycomics; glycoproteomics; gangliosides; sialylation; mass spectrometry

Introduction

HDL particles have been considered to be atheroprotective due to their role in reverse cholesterol transport, however, many other functions including toxin binding, antioxidant, anti-inflammatory, antiglycation, antithrombotic, and immunomodulatory functions have recently been described.[1] HDL particles are heterogeneous, and yet the molecular and functional bases behind the large degree of variability among the different classes and subclasses of HDL particles have not been established.[2] A key challenge facing the field of lipoprotein biology is that chemical, compositional, and structural changes can transform atheroprotective HDL into pro-atherogenic, pro-inflammatory particles.[3] Under

To whom correspondence should be addressed Carlito B. Lebrilla cblebrilla@ucdavis.edu. Tel: 01-530-752-6465 Fax: 01-530-752-8995..

inflammatory conditions HDL particles are ineffective at reverse cholesterol transport despite high plasma HDL concentrations.[4] The anti-oxidant function of HDL –protection of LDL from oxidation– is impaired in heart disease patients.[5] Dysfunctional HDL with impaired anti-oxidant and endothelial protection are found in type 2 diabetes patients.[6] HDL from patients with cardiovascular disorders are compositionally different from those of healthy individuals.[7, 8] In addition, the antimicrobial, anti-inflammatory, antiglycation, antithrombotic, and immunomodulatory functions of HDL and how these are modified by HDL composition are poorly understood.

As complex multi-molecular aggregates, many of the functional proteins and lipids in HDL are potentially glycosylated. Yet, very little is known about these glycoconjugates of HDL. There is evidence that ApoA-I, A-II, C-I, C-II, and C-III are all glycosylated.[9] Glycosylation of ApoA may be important for the secretion of HDL from the liver[10], and may influence its association/dissociation properties to HDL particles: sialylated ApoA-II associated only with HDL_3 whereas non-sialylated ApoA-II associated with HDL of all sizes.[11] Desialylation of ApoE is associated with hepatic steatosis.[12] ApoE Leiden, an aberrantly glycosylated variant of ApoE, shows defective binding to the LDL receptor.[13] Decreased sialic acid in cerebrospinal fluid ApoE was found with aging, and was associated with smaller lipoprotein particle sizes, which may be involved in the formation of amyloid plaque.[14] Loss of sialic acid α2,6-Neu5Ac containing structures in ApoC-III was found in lung cancer patients.[15] Serum amyloid A (SAA), which is released in response to acute phase immune reaction circulates primarily as a constituent of HDL particles.[16] An N-glycosylated form of SAA that is distinct from acute phase SAA has been described.[17] These data suggest important as yet not fully characterized mechanistic links between the glycosylation of HDL-associated glyocoproteins and HDL function. However, the glycosylation of the HDL proteome has not been characterized.

Gangliosides are glycolipids containing sialic acids in their carbohydrate moieties. Bacterial toxins display a heterogeneous specificity of binding to their glycolipid receptors.[18] For example, lactosylceramide and ganglioside GM3 bind several enterotoxigenic strains of *E. Coli*.[19] Twenty-five percent of serum gangliosides were reported to be associated with HDL in human serum, with a different compositional profile for HDL compared with other circulating lipoproteins (e.g. VLDL and LDL) and serum.[20] However, only limited information is available on the occurrence of these ganglioside species in plasma HDL, and whether and how they vary with disease.

Studies of the HDL proteome have uncovered an array of 110 proteins that are thought to be associated with HDL particles. In fact, it is now thought that different subsets of HDL particles, separated in different ways – ultracentrifugation, electrophoretic migration, immunoaffinity chromatography, size exclusion chromatography, and others – are characterized by different proteomes.[21] However, although the proteins that associate with HDL have been identified and for some of these proteins the glycosylation has been characterized independently, to date, there have been no direct investigations of the overall glycome of HDL.

In this article we describe an analytical strategy that is detailed and quantitative, comprehensively examining the glycan structures on glycoproteins and glycolipids of HDL. Previously, no adequate methods to determine HDL glycan diversity as a whole in a clinically relevant manner existed. Methods for elucidating the complete HDL glycome using a combination of nanoflow liquid chromatography and high performance mass spectrometry for the simultaneous identification and quantification of glycoconjugates in HDL particles are described. On the basis of the glycosylation discovered we propose a new model for HDL as a class of highly sialylated particles.

Experimental Procedures

A comprehensive glycome analysis work-flow is summarized in Figure 1 and described below.

HDL Isolation

Fasting (12 hr) blood samples were obtained from a healthy study participant as part of an ongoing approved protocol to collect fasting plasma from healthy subjects for methods development. Briefly, healthy subjects are recruited on the University of California Davis campus by flyering and announcements at seminars. Subjects are screened for basic eligibility criteria (healthy, able to give blood, and not taking any medications) and provide written informed consent to participate in the study. The Institutional Review Board of the University of California Davis approved the study protocol. The study was conducted according to the principles expressed in the Declaration of Helsinki.

Preparation of HDL was performed by a sequential micro-ultracentrifugation method described by Brousseau et al.[22] with slight modifications. Blood was collected from the antecubital vein into EDTA evacuated tubes, centrifuged immediately (1,300 ×g, 10 min, 4°C), portioned into aliquots, and stored at –80 °C until analyzed. Three thawed replicate plasma samples (0.8ml each as triplicates) were gently overlaid on the KBr solution to avoid the introduction of air. To isolate the combined VLDL and LDL fractions, potassium bromide (KBr) solution (1.1 ml, d = 1.084 g/ml) was transferred into cone-top polyallomer tubes up to the 1.9ml neckline. Ultracentrifugation was performed using a Sorvall RC M120 GX equipped with a S120-AT2 fixed-angle rotor (Thermo Scientific, Waltham, MA, USA) for 2.5 h, 8°C, 435,680 ×g. By this procedure the combined VLDL and LDL fractions with a density lower than 1.060 g/mL were removed from the top of the tubes (0.9 ml) by aspiration using a gel-loading pipette (Rainin, Oakland, CA, USA). The remaining infranate (1.0 ml) was transferred into new cone-top polyallomer tubes. To isolate the HDL fraction, the transferred infranate was overlaid with 0.9ml of KBr solution (d = 1.34 g/ml) and ultracentrifugation was performed (3 hr, 8°C, 435,680 ×g). The HDL fraction (1.2 g/ml-1.063) was identified as the top 0.6ml layer found at the top of the tubes. The HDL fraction was collected from the top of the tube (0.6 ml) and desalted using an Amicon dialysis membrane with a molecular weight cut-off of 3,000 (Millipore, Billerica, MA, USA) in nanopure water (18 Ω), prior to being dried down and reconstituted with 300 μL water.

Density solutions of KBr, at d = 1.084 g/ml and 1.34 g/ml were made weekly and adjusted and verified by measurement using the Densito 30PX portable densitometer (Mettler Toledo, Columbus, OH, USA). Thirteen replicates of plasma samples isolated from fasted and fed healthy human subjects were measured by the Densito 30PX to verify the density of plasma. The mean ± SEM density of the plasma samples was 1.027 ± 0.0005 g/ml.

Glycoprotein Analysis

Tryptic Digestion—100 μL of 50 mM ammonium bicarbonate solution was added to 10 μL isolated HDL, followed by reducing with 5 μL of 550 mM dithiothreitol (DTT) with incubation for 50 min at 60 °C. 10 μL of 450 mM iodoacetamide (IAA) was then added and carboxymethylation was performed by incubation for 20 min at room temperature in dark. Reduced and carboxymethylated HDL was digested using Sequencing Grade Modified Trypsin (Promega, Madison, WI, USA) 2 μL (1 μg/μL) in 100 μL of 50 mM ammonium bicarbonate buffer , for 16 hr at 37 °C. The digests were purified on a reverse-phase cleanup C18 pipette tip (Agilent Technology, Wilmington, DE, USA). The C18 zip-tip was preconditioned successively with acetonitrile (150 μL, 10 times) and water (150 μL, 10

times). The tryptic digest was loaded on to the zip-tip by pipetting 20 times up and down and then washed with water (150 μL) for 10 times. HDL tryptic peptides were eluted with 0.05% formic acid (FA) in 80% acetonitrile (ACN) in water (v/v) (200 μL, 20 times extractions), dried down, and then reconstituted in 20 μL nanopure water.

N-linked Glycan Release and Purification—N-linked glycans were released from 60 μL HDL in 200 μL 100mM ammonia bicarbonate buffer using endoglycosidase PNGase F (New England Biolabs, Ipswich, MA, USA) (2 μL) for 10 min under microwave condition (power 20 W, temperature 60 °C). The released N-glycans were cleaned up via solid phase extraction (SPE) using graphitized carbon cartridges (Grace Davison Discovery Sciences, Deerfield, IL, USA). The glycan digest was loaded on preconditioned graphitized carbon cartridges then washed with 6 mL nanopure water. N-glycans were eluted with 6 mL 0.05% Trifluoroacetic acid (TFA) in 40% ACN in water (v/v), dried down, prior to reconstituted in 20 μL nanopure water for MS analysis.

Pronase Digestion and Glycopeptide Cleanup—100 μg Pronase E was covalently coupled to cyanogen bromide (CNBr) activated sepharose beads (Sigma-Aldrich, St. Louis, MO, USA) via coupling chemistry and as earlier reported in our laboratory.[23-26] 100 μL isolated HDL was added to the Pronase-beads and incubated at 37 °C for 18 h. Pronase would normally digest the glycoproteins to glycopeptides with peptide portion 1-20 amino acids. The glycopeptide digest was desalted and enriched via SPE procedure using graphitized carbon cartridges. Similar as N-glycan cleanup procedure, followed by conditioning the cartridges using acetonitrile and water and loading the digest mix, a clean mixture of glycopeptides were eluted in 9 mL 0.05% Trifluoroacetic acid (TFA) in 40% ACN in water (v/v), dried down, and then reconstituted in 20 μL nanopure water prior to MS analysis.

Ganglioside Analysis

Extraction of Gangliosides—100 μL isolated HDL was mixed with 1 mL water, 2.7 mL methanol and 1.3 mL chloroform and the mixture was shaken vigorously for 5 seconds. After centrifugation at 3,000 g for 5 min, 0.5 mL of water was added for the phase separation. The supernatant was collected. The bottom organic layer was re-extracted using 5 mL of 3:4:8 water/chloroform/methanol (v:v:v) and mixed, and then the supernatants were pooled and dried.

A C8 SPE cartridge (Supelco, Bellefonte, PA, USA) was conditioned with 6mL of 1:1 isopropanol/methanol (v/v) and 1:1 methanol/water (v/v). The sample was diluted with 1mL of 1:1 methanol/water (v/v) and applied on the SPE cartridge. The cartridge was washed with the 9mL of 1:1 methanol/water (v/v) solution to ensure removal of all polar compounds. The gangliosides were eluted by washing 9mL of 1:1 isopropanol/methanol (v/v), and the eluant was evaporated to dryness. The purified sample was stored at −80 °C until analysis.

Instrumentation

A nano-HPLC-Chip Q-TOF instrument using the Agilent 1200 series microwell-plate autosampler (maintained at 6 °C by the thermostat), capillary pump, nano pump, HPLC-Chip interface, and the Agilent 6520 Q-TOF MS (Agilent Technologies, Inc., Santa Clara, CA) was used in this study.

For the tryptic peptide and the ganglioside analyses, a reverse-phase nano-HPLC Chip (G4240-62001, Agilent Technologies, Inc., Santa Clara, CA) with a 40 nL enrichment column and 43 × 0.075 mm ID analytical column was used. The column was packed with

ZORBAX C18 (5 μm pore size) stationary phase. The mobile phase for tryptic peptides consisted of 0.1% formic acid in 3% ACN in water (v/v) as solvent A, and 0.1% formic acid in 90% ACN in water (v/v) as solvent B. The mobile phases used for gangliosides were water (solvent C) and 15% isopropanol in methanol (v/v) (solvent D), with both containing 20 mM ammonium acetate and 0.1% acetic acid. The nano pump gradient was performed on the analytical column to separate the tryptic peptides with a flow rate at 0.4 μL /min and the gangliosides with 0.3 μL /min. The peptides were eluted in 45 min with the following gradient: 0% B (0.00-2.50 min); 0 to 16% B (2.50-20.00 min); 16 to 44% B (20.00-30.00 min); 44 to 100% B (30.00-35.00 min) and 100% B (35.00 -45.00 min). The gradient used for gangliosides separation was as follows: 70% of D (0.00-1.00 min); 70 to 80% D (1.00-3.00 min); 80 to 100% D (3.00-40.00 min) and 100% D (40.00-45.00 min). The working samples were dissolved in water/methanol (1:1, v/v).

For the N-glycan and the pronase glycopeptide analysis, an Agilent 6210 HPLC Chip II with a 40 nL enrichment column and 43 × 0.075 mm ID analytical column both packed with porous graphitized carbon stationary phase was used. The mobile phase consisted of 0.1% formic acid in 3% ACN in water as solvent A and 0.1% formic acid in 90% ACN in water (v/v) as solvent B. The nano pump gradient was performed on the analytical column to separate the N-glycans and glycopeptides with a flow rate at 0.4 μL /min. The samples were eluted in 45 min with the following gradient: 0% B (0.00-2.50 min); 0 to 16% B (2.50-20.00 min); 16 to 44% B (20.00-30.00 min); 44 to 100% B (30.00-35.00 min) and 100% B (35.00-45.00 min).

The Agilent 6520 Q-TOF MS was operated in the positive ion mode for MS and MS/MS modes for the tryptic peptides, N-glycans, and pronase glycopeptides. The recorded mass ranges were m/z 500-3,000 for MS only and m/z 50-3,000 for MS/MS. Acquisition rates were 0.63 spectra/s for both MS and MS/MS. For gangliosides, MS was operated in the negative and MS/MS was operated in both positive and negative modes. The recorded mass ranges were *m/z* 500-2,500 for MS only and *m/z* 50-1,500 for MS/MS. The drying gas temperature was set at 325 °C with a flow rate of 4 L/min. All mass spectra were internally calibrated using the G1969-85000 ESI tuning mix (Agilent Technologies, Inc., Santa Clara, CA), with reference masses at *m/z* 922.010, and 1,521.971 in the positive ion mode, at *m/z* 680.036 and 1279.995 for negative mode.

In MS/MS mode, generally, the collision energies for the tryptic peptides, N-glycans, and pronase glycopeptides were calculated as:

$$V_{\text{collision}} = 3.6V\left(\frac{\text{m/z}}{100\text{Da}}\right) - 4.8\text{V}\,(\text{tryptic peptides})$$
$$V_{\text{collision}} = 1.8\text{V}\left(\frac{\text{m/z}}{100\text{Da}}\right) - 4.8\text{V}\,(\text{N-glycans and pronase glycopeptides})$$

For gangliosides, the data dependent MS/MS analysis was performed with collision energies set at 40V for the negative mode and 80V for the positive mode.

Data Analysis

All tryptic MS/MS data were analyzed using X! Tandem (www.thegpm.org). Trypsin digesion would help ID the HDL associated proteins. X! Tandem was set up to search the Swissprot human complete proteome set database. X! Tandem was searched with a fragment ion mass tolerance of 80 ppm and a parent ion tolerance of 100 ppm. Iodoacetamide derivative of cysteine was specified in X! Tandem as a fixed modification. Deamidation of asparagine and glutamine, oxidation of methionine and tryptophan were specified in X! Tandem as variable modifications

Data analyses for N-glycans, glycopeptides and gangliosides were performed with the MassHunter Qualitative Analysis software ver. B.03.01 (Agilent Technologies, Inc., Santa Clara, CA).

For the N-glycan analysis, within a 20 ppm accurate mass criterion molecular Feature Extraction (MFE) was performed through a mode of the “Find by Molecular Feature” function for non-targeted profiling. The deconvoluted glycan mass, retention time, and the abundance were extracted. The glycan compositions were assigned based on the accurate mass and the corresponding MS/MS data.

Glycopeptide assignments were achieved by the combination of the tandem MS information and the accurate glycopeptide precursor ion mass via in-house software GP Finder. The mass list of the glycopeptides precursor ions was analyzed with accurate mass, protein sequence, biological filters of glycans, and a MS tolerance level (≤20 ppm). The tandem mass spectra were then taken into account for further inspection with glycan and peptide fragmentation patterns with a mass tolerance for fragment ions (≤80 ppm). The unique significance of GP Finder is to use false discovery rate by generating a decoy library to the scoring system and to serve as a more reliable means of making assignments.

For gangliosides, MFE was performed to generate a peak list (*m/z*, retention time and peak area) taking all ions into account exceeding 1,000 counts. Focused post-processing precursor ion scan analysis was performed through a mode of the “Find by Auto MS/MS”. The NeuAc ions (m/z 290.095) were the fragment ions used to determine the precursor ion masses representing gangliosides.

Results and Discussion

HDL particles remain poorly characterized due to their size, complexity, dynamic nature and large degree of diversity in composition and function. Enabling technologies that can be used to comprehensively analyze these biologically important particles are needed. In particular, very little is known about the biological functions related to the glycosylated components of HDL. This deficiency in understanding the glycobiology of HDL may be critically important since early published evidence indicates that both glycoproteins and glycolipids associated with HDL and their variation in glycosylation patterns may be either mechanistically involved or diagnostic of HDL functions. In this study HDL particles isolated from healthy human plasma were comprehensively examined for their glycan structures and the results lead to a compelling new model of HDL as a class of highly sialylated particles.

Proteomics Analysis

Tryptic peptides were digested from HDL fractions isolated by ultracentrifugation. After high-performance liquid chromatography (HPLC) separation via reversed phase C18 column, the peptides were analyzed by tandem MS. Following database search, 17 proteins were identified shown in Supplemental Table S1 from one replicate as an example. The base −10 log of the expectation that any particular protein assignment was made at random was lower than −2. ApoA-I was observed as the major protein. In humans, about 60% of the protein content in HDL is represented by ApoA-I.[27] Other apoproteins were present, including Apo C-II, C-III, D, E, and M, which are typical minor apoproteins associated with HDL. On the other hand, ApoB-100, the major constituent of VLDL and LDL, was not present. Other proteins known to be associated with HDL were also observed, including acute phase response proteins such as SAA, liver secreted proteins such as alpha-2-HS-glycoprotein (fetuin A), and the key mediators of the complement system C3 inhibitor. [28-31] The proteins associated with HDL isolated from healthy human plasma in this study

have all been suggested as HDL-associated proteins in previous studies.[32-35] These results confirmed our HDL isolation approach, and provided a list of proteins for site-specific glycosylation analysis.

Glycans from HDL compositionally profiled by Nano-LC MS

The N-glycans were released using the protocol described in experimental procedures. Analyses were done from the isolated HDL triplicates. The glycan profile of HDL is illustrated with one of the triplicates (Figure 2). The depicted glycan structures were based on biological precedence and their correct masses, however, isomers are putative.[36] HPLC-microchip packed with a PGC stationary phase was used to separate glycans with high sensitivity and reproducibility.[37-40] The total ion chromatogram (TIC) from the raw LC/MS data was separated into a number of extracted compound chromatograms (ECCs). The extractor algorithm was based on the expected charge carriers, potential neutral mass losses, and a predicted isotopic distribution. Each peak represents one compound eluting at certain retention time with the detected m/z, which enables the assignments of glycan composition.

The most abundant glycan (including isomers) was a biantennary complex type glycan with two sialic acids ($Hexose_5HexNAc_4Neu5Ac_2$). Perhaps not surprisingly, these glycans are also the most abundant in blood.[36] In this regard, HDL-associated proteins are similar to other abundant glycoproteins in blood.[41] Two abundant isomers were observed eluting at retention times 23 min and 25 min. Most of the glycans (90%) from HDL glycoproteins were sialylated with one or two Neu5Ac(s). Ion intensities were measured in the MS mode based on the protonated molecular ion in positive mode (Table 1). Following the most abundant glycan with two Neu5Ac, a complex type biantennary glycan with one Neu5Ac was shown in a high intensity eluting at 17 min – 20 min including four observed isomers. Our group reported glycans with sialic acids retain longer with PGC.[39] Here we also observed that the sole addition of an acidic NeuAc residue increased the retention time by nearly 5 min.

Sialic acid, mostly found as a terminal component of glycoproteins and glycolipids on the outer surface of cells, is involved in cellular secretions.[42] Sialic acid participates in multiple and diverse cellular events, such as acting as an antirecognition agent by shielding recognition sites[42-44] and conversely by being a biological recognition site as a ligand for multiple molecules.[45, 46] Sialic acid is anionic and therefore likely contributes to HDL's negative charge. Previously it has been shown that the addition of phosphatidylinositol, which increases HDL's negative charge, blocked binding of HDL to hepatic lipase.[47] Other previous studies have also shown that the electronegativity of HDL affects its binding to cholesterol ester transfer protein and thus the exchange of cholesterol esters with LDL.[48] The sialylated glycans in HDL associated proteins may be involved in molecular and cellular interactions that affect the function of HDL. For example, sialic acid residues of ApoE may be essential for its recognition by HDL_3 particles and further the binding to HDL_3.[49] Interestingly, desialylation of lipoprotein-associated apoproteins was found to be associated with increased circulating neuraminidase excreted by *Streptococcus pneumonia* in patients with hemolytic uremic syndrome,[50] suggesting that bacterial infection may lead to desialylation of HDL particles *in vivo*.

In addition to complex type sialylated N-glycans, fucosylated N-glycans were present at relatively low abundances. High-mannose and hybrid type N-glycans were also observed, indicating the variety of N-glycans from HDL-associated proteins. The wide dynamic range of the detected N-glycans by the described method allows the evaluation of all types of oligosaccharides and further analyses of their biological functions.

Supplemental Figure S1 shows the overlaid ECCs of N-glycans from the three replicates. The separation of glycans and their profiles was similar, as the most abundant ones were observed as sialylated complex type eluting at 23 min-25 min. The method is considered reproducible with regard to the glycan composition assignments from these technical triplicates.

Site-specific analysis of HDL Glycoproteins

Glycopeptides were assigned based on a combination of the MS/MS data and the accurate precursor ion mass measurement. The advantage of non-specific digestion with pronase is the ability of the enzyme mixture to cleave the protein(s) into short peptides with typically one glycosylation site. Previous studies from our group on the analysis of non-specific digested glycopeptides with CID (collision-induced dissociation) experiments revealed detailed and comprehensive glycan compositional information for each glycopeptide (both N- and O-linked).[23, 24] Glycosidic bond cleavages (B- and Y- type ions) were the major products as well as some minor peptide fragmentations.

Table 2 lists the pronase digested glycopeptides from HDL associated glycoproteins with their glycan composition, glycosylation site, protein ID, and intensity. The most abundant N-glycan ($Hexose_5HexNAc_4Neu5Ac_2$) was found in multiple glycoproteins from the glycopeptide assignment. Here, all the identified proteins from the HDL were confirmed in triplicate experiments using X! Tendem and were used in the glycopeptide assignment search. A number of deconvoluted glycopeptide MS/MS spectra are shown as examples in Figure 3. Figure 3A represents the MS/MS spectrum for a triprotonated fetuin A glycopeptide containing this most abundant disialylated N-glycan. Particularly unique to glycopeptides containing sialylated glycans are B-type ions corresponding to neutral mass 291 Da (Neu5Ac), and neutral mass 273 Da ($Neu5Ac–H_2O$). Mass peaks also include those observed as 203 Da, 365 Da, and 656 Da, which correspond to the neutral masses of HexNAc, (Hex+HexNAc), and (Hex+HexNAc+Neu5Ac). Due to the labile nature of sialic acid residues and their positions at the termini, the initial loss of sialic acid was commonly observed with the sialylated glycopeptides. Following the sequential neutral losses of monosaccharides of Neu5Ac, Hexose and HexNAc, the CID data revealed the mass peak 832 Da corresponding to glycopeptide (APLNDT+HexNAc). The presence of (peptide +HexNAc) is considered a valuable means for validating the assignment of glycopeptide particularly when analyzing complex protein mixtures.[51]

Pronase digestion simultanously enables site-specific analysis of both N- and O-glycans. In addition to the abundant N-glycans discussed previously, a number of O-glycopeptides were present attached with sialylated O-glycans (Table 2). The observed O-glycans associated with the HDL glycoproteins were all sialylated, comfirming that HDL particles are highly sialylated. Figure 3(B and C) revealed the deconvoluted MS/MS spectra for two diprotonated O-glycopeptides from ApoC-III and fetuin A, respectively. Most O-glycopeptides analyzed in the HDL mixture contained a core 1 type with two Neu5Acs.

Figure 4 shows the site heterogeneity of four glycoproteins from eight of the identified HDL associated glycoproteins as an example. Fetuin A is a multifunctional circulating liver-derived glycoprotein in serum and plasma.[52] Several studies have suggested that fetuin A may be critically important to cardiovascular health.[53-56] Both N- and O-glycans were observed at multiple glycosylation sites with fetuin A, all of which were sialylated (Figure 4A), which is consistent with the previous glycosylation analysis on the individual protein fetuin A.[57] The most abundant glycan ($Hexose_5HexNAc_4Neu5Ac_2$) was disialylated and was found on most of the glycoproteins examined. It was present at ASN^{156} and ASN^{176} of fetuin A.

Angiotensinogen is a heterogeneous glycoprotein mainly produced by hepatocytes in plasma, which has a well-known role in blood pressure regulation in animals and humans.[58] It has previously been shown that the glycosylation of angiotensinogen may play a significant role in its functional heterogeneity.[59] Results of site heterogeneity of angiotensinogen are summarized in Figure 4B. Among the four potential N-glycosylation sites, three identified sites were occupied with N-glycans in this study. While two sites were observed associated with sialylated N-glycans, site ASN^{304} was attached with fucosylated N-glycans. Angiotensinogen was also found attached with the most abundant sialylated glycan ($Hexose_5HexNAc_4Neu5Ac_2$) at ASN^{170}.

Figure 4C details the glycan associated with Alpha-1B-glycoprotein (A1BG). A1BG is believed to be a member of the immunoglobulin family.[60]The mono-sialylated glycan ($Hexose_5HexNAc_4Neu5Ac_1$) attached at ASN^{363} on A1BG.

The glycosylation of apolipoprotein C3 (Apo C3) was analyzed by a couple of groups, showing the distribution of O-glycans.[61, 62] The disialylated O-glycan at site Thr^{94} from ApoC-III is shown in Figure 4D. APO C3 inhibits lipoprotein lipase and hepatic lipase, thought to inhibit hepatic uptake of triglyceride-rich particles.[63] APO C3 was also recently found to be increased in HDL isolated from patients with both stable coronary artery disease and acute coronary syndrome as well as in hemodialysis patients.[64, 65]

In general, for the first time the site-specific glycosylation of these proteins in HDL particles has been described. Compared with previous disscussed glycan analysis, there were some glycans that were not observed in the glycopeptide analysis due to their low abundances as well as the potential short peptide length from pronase digestion. However, the functions they impart on HDL through their glycosylation, and whether alterations in their glycosylation as part of HDL particles is either causative or diagnostic in disease are unknown.

HDL gangliosides characterized by MS/MS

Gangliosides are another contributor of sialic acid in HDL. We applied a high resolution Q-TOF MS method with reverse-phase nanoHPLC separation for the analysis of human HDL gangliosides. The high mass accuracy of these instruments, along with the MS/MS capability made it possible to perform focused detection of ganglioside species in the polar lipid extract.[66] Post-processing precursor ion scans indicate the existence of gangliosides, which elute at certain retention times. Moreover, based on accurate mass, glycan information and ceramide composition were simultaneously obtained.

Figure 5 is representative of the extracted compound chromatograms (ECCs) of HDL gangliosides. The chromatogram reveals an elution pattern starting with gangliosides with shorter ceramide chains followed by those with longer ceramides. Examination of the profiles shows that GM3 (monosialoganglioside, NeuAc2-3Gal1-4Glc-Cer) and GD3 (disialoganglioside, NeuAc2-8NeuAc2-3Gal1-4Glc-Cer) were abundant ganglioside ions in HDL from healthy human plasma, in agreement with earlier studies.[67] Eight GM3 and four GD3 gangliosides were detected. A 60% GM3 and 40% GD3 distribution was observed, and ion intensities were measured in the MS mode based on the deprotonated molecular ion (Table 3). Interestingly, the composition of human aorta from patients who had died of myocardial infarction were found to have higher GD3 content in the aortic media versus the intima[68] and total ganglioside content was found to be lower in cells isolated from atherosclerotic compared with normal human aorta.[69] Gangliosides have even been found to stimulate lipoxygenase-mediated eicosanoid production in peripheral blood lymphocytes, and GD3 was more stimulatory compared with GM1 or GM3.[70] These previous reports suggest that ganglioside content and composition may have

important biological implications in heart disease and its related mechanisms involving lipoproteins.

The analysis also revealed the composition of the major ceramide portion of GM3 and GD3 gangliosides. Both GM3 and GD3 were composed of heterogeneous ceramide lipid tails, including d18:1/16:0 and d18:1/23:0. Types of sphingoid bases and fatty acids in the backbones were determined with the use of 80V MS/MS. Fragments at *m/z* 264.269 and at *m/z* 236.238 indicated the existence of sphingoid bases d18:1 and d16:1, respectively. As an example, GM3 (d18:1/16:0) yields a diagnostic sialic acid fragment at *m/z* 290.09 in 40V negative mode MS/MS, while 80V positive mode MS/MS spectrum provides the ceramide information at *m/z* 520.49 and 264.27 (Supplemental Figure S2). The importance of the ceramide lipid tail compositional differences is currently poorly understood. For example, transmembrane anchored angiotensin converting enzyme, an enzyme important for blood pressure regulation, was found to associate only with C18 but not C16 sphingomyelin containing rafts.[71] A recent report showed that nascent HDL resemble lipid rafts suggesting the possibility that HDL have microheterogeneity with lipid raft-like portions of the phospholipid outer layer that recruit specific gangliosides and proteins to perform specific functions, just as occurs in plasma membrane lipid rafts.[72] The simultaneous identification of the glycan and ceramide will provide a clearer picture of the role of gangliosides in lipoprotein biology.

Conclusion

We have established analytical methods for profiling the glycome of HDL particles. the approach detailed here provides a simultaneous and detailed analysis of glycoproteins (both N-and O-glycan composition, as well as site-specific glycopeptide composition) and gangliosides (both the glycan and ceramide portion) that was previously not achievable. The methods developed in this study can be used for the analysis of other nanobioparticles including LDL, VLDL, and chylomicrons, as well as the various size subclasses of these major lipoprotein classes. This approach will have implications for elucidating a number of biological functions of HDL. With this method in place it is now possible to conduct an array of experiments and analyses of clinical samples to understand the important biological functions and diagnostic potential of HDL that are mediated by glycans.

Supplementary Material

Refer to Web version on PubMed Central for supplementary material.

Acknowledgments

The study was funded by grants from the National Institutes of Health (R01GM049077) and the University of California Discovery Program (BIO08-128504 and 09 GEB-02 NHB) the California Dairy Research Foundation.

Abbreviations

HDL	high density lipoprotein
LDL	low density lipoprotein
VLDL	very low density lipoprotein
APO	apoprotein
HPLC	high-performance liquid chromatography
Q-TOF	quadrupole time-of-flight

CID	collision-induced dissociation
SPE	solid phase extraction
Hex	hexose
HexNAc	N-acetylhexosamine
Neu5Ac	neuraminic acid (sialic acid)
Fuc	fucose
GCC	graphitized carbon cartridge
PNGase F	peptide N-glycosidase F
ACN	acetonitrile

Reference

1. Soran H, et al. HDL functionality. Curr Opin Lipidol. 2012; 23(4):353–66. [PubMed: 22732521]
2. Asztalos BF, Tani M, Schaefer EJ. Metabolic and functional relevance of HDL subspecies. Curr Opin Lipidol. 2011; 22(3):176–85. [PubMed: 21537175]
3. Ansell BJ, Fonarow GC, Fogelman AM. The paradox of dysfunctional high-density lipoprotein. Curr Opin Lipidol. 2007; 18(4):427–34. [PubMed: 17620860]
4. Sviridov D, et al. Elevated HDL cholesterol is functionally ineffective in cardiac transplant recipients: evidence for impaired reverse cholesterol transport. Transplantation. 2006; 81(3):361–6. [PubMed: 16477221]
5. McMahon M, et al. Dysfunctional proinflammatory high-density lipoproteins confer increased risk of atherosclerosis in women with systemic lupus erythematosus. Arthritis Rheum. 2009; 60(8): 2428–37. [PubMed: 19644959]
6. Van Linthout S, et al. High-density lipoprotein at the interface of type 2 diabetes mellitus and cardiovascular disorders. Curr Pharm Des. 2010; 16(13):1504–16. [PubMed: 20196738]
7. Vaisar T, et al. HDL in humans with cardiovascular disease exhibits a proteomic signature. Clin Chim Acta. 2010; 411(13-14):972–9. [PubMed: 20307520]
8. Park KH, et al. The functional and compositional properties of lipoproteins are altered in patients with metabolic syndrome with increased cholesteryl ester transfer protein activity. Int J Mol Med. 2010; 25(1):129–36. [PubMed: 19956911]
9. Jin Y, Manabe T. Direct targeting of human plasma for matrix-assisted laser desorption/ionization and analysis of plasma proteins by time of flight-mass spectrometry. Electrophoresis. 2005; 26(14): 2823–34. [PubMed: 15934056]
10. Lee J, et al. Hyperexpression of N-acetylglucosaminyltransferase-III in liver tissues of transgenic mice causes fatty body and obesity through severe accumulation of Apo A-I and Apo B. Arch Biochem Biophys. 2004; 426(1):18–31. [PubMed: 15130779]
11. Remaley AT, et al. O-linked glycosylation modifies the association of apolipoprotein A-II to high density lipoproteins. J Biol Chem. 1993; 268(9):6785–90. [PubMed: 8454651]
12. Massey JB. Kinetics of transfer of alpha-tocopherol between model and native plasma lipoproteins. Biochim Biophys Acta. 1984; 793(3):387–92. [PubMed: 6424717]
13. Fazio S, et al. Preferential association of apolipoprotein E Leiden with very low density lipoproteins of human plasma. J Lipid Res. 1993; 34(3):447–53. [PubMed: 8468528]
14. Kawasaki K, et al. Sialic acid moiety of apolipoprotein E and its impact on the formation of lipoprotein particles in human cerebrospinal fluid. Clin Chim Acta. 2009; 402(1-2):61–6. [PubMed: 19138682]
15. Ueda K, et al. Targeted serum glycoproteomics for the discovery of lung cancer-associated glycosylation disorders using lectin-coupled ProteinChip arrays. Proteomics. 2009; 9(8):2182–92. [PubMed: 19322776]

16. Cabana VG, et al. Influence of apoA-I and apoE on the formation of serum amyloid A-containing lipoproteins in vivo and in vitro. J Lipid Res. 2004; 45(2):317–25. [PubMed: 14595002]
17. Whitehead AS, et al. Identification of novel members of the serum amyloid A protein superfamily as constitutive apolipoproteins of high density lipoprotein. J Biol Chem. 1992; 267(6):3862–7. [PubMed: 1740433]
18. O'Gorman RB, et al. Correlation of immunologic and nutritional status with infectious complications after major abdominal trauma. Surgery. 1986; 99(5):549–56. [PubMed: 3704913]
19. Sanchez-Juanes F, et al. Glycosphingolipids from bovine milk and milk fat globule membranes: a comparative study. Adhesion to enterotoxigenic Escherichia coli strains. Biol Chem. 2009; 390(1): 31–40. [PubMed: 18937626]
20. Senn HJ, et al. Gangliosides in normal human serum. Concentration, pattern and transport by lipoproteins. Eur J Biochem. 1989; 181(3):657–62. [PubMed: 2731542]
21. Vaisar T. Proteomics investigations of HDL: challenges and promise. Curr Vasc Pharmacol. 2012; 10(4):410–21. [PubMed: 22339300]
22. Brousseau T, et al. Sequential ultracentrifugation micromethod for separation of serum lipoproteins and assays of lipids, apolipoproteins, and lipoprotein particles. Clinical chemistry. 1993; 39(6): 960. [PubMed: 8504564]
23. Hua S, et al. Site-specific protein glycosylation analysis with glycan isomer differentiation. Analytical and Bioanalytical Chemistry. 2012; 403(5):1291–1302. [PubMed: 21647803]
24. Nwosu CC, et al. Simultaneous and Extensive Site-specific N- and O-Glycosylation Analysis in Protein Mixtures. Journal of Proteome Research. 2011; 10(5):2612–2624. [PubMed: 21469647]
25. Seipert RR, et al. Anal. Chem. 2008; 80(10):3684. [PubMed: 18363335]
26. Seipert RR, Dodds ED, Lebrilla CB. J. Proteome Res. 2009; 8(2):493. [PubMed: 19067536]
27. Hedrick CC, et al. In vivo interactions of apoA-II, apoA-I, and hepatic lipase contributing to HDL structure and antiatherogenic functions. Journal of Lipid Research. 2001; 42(4):563–570. [PubMed: 11290828]
28. Baumann M, et al. Association between carotid diameter and the advanced glycation endproduct Nepsilon-Carboxymethyllysine (CML). Cardiovascular Diabetology. 2009; 8(1):45. [PubMed: 19660101]
29. Sakwe AM, et al. Fetuin-A (α2HS-Glycoprotein) Is a Major Serum Adhesive Protein That Mediates Growth Signaling in Breast Tumor Cells. Journal of Biological Chemistry. 2010; 285(53):41827–41835. [PubMed: 20956534]
30. Jensen LE, Whitehead AS. Regulation of serum amyloid A protein expression during the acute-phase response. Biochemical Journal. 1998; 334(3):489–503. [PubMed: 9729453]
31. Rezaee F, et al. Proteomic analysis of high-density lipoprotein. PROTEOMICS. 2006; 6(2):721–730. [PubMed: 16419016]
32. Gordon S, et al. High-Density Lipoprotein Proteomics: Identifying New Drug Targets and Biomarkers by Understanding Functionality. Curr Cardiovasc Risk Rep. 2010; 4(1):1–8. [PubMed: 20625533]
33. Hortin GL, et al. Diverse range of small peptides associated with high-density lipoprotein. Biochem Biophys Res Commun. 2006; 340(3):909–15. [PubMed: 16386709]
34. Karlsson H, et al. Lipoproteomics II: mapping of proteins in high-density lipoprotein using two-dimensional gel electrophoresis and mass spectrometry. Proteomics. 2005; 5(5):1431–45. [PubMed: 15761960]
35. Subramaniyam D, et al. C-36 peptide, a degradation product of alpha1-antitrypsin, modulates human monocyte activation through LPS signaling pathways. Int J Biochem Cell Biol. 2006; 38(4):563–75. [PubMed: 16384723]
36. Aldredge D, et al. Annotation of a Serum N-Glycan Library for Rapid Identification of Structures. Journal of Proteome Research. 2012; 11(3):1958–1968. [PubMed: 22320385]
37. Hua S, et al. Comprehensive native glycan profiling with isomer separation and quantitation for the discovery of cancer biomarkers. Analyst. 2011; 136(18):3663–3671. [PubMed: 21776491]

38. Nwosu CC, et al. Comparison of the Human and Bovine Milk N-Glycome via High-Performance Microfluidic Chip Liquid Chromatography and Tandem Mass Spectrometry. Journal of Proteome Research. 2012; 11(5):2912–2924. [PubMed: 22439776]
39. Chu CS, et al. Profile of native N-linked glycan structures from human serum using high performance liquid chromatography on a microfluidic chip and time-of-flight mass spectrometry. PROTEOMICS. 2009; 9(7):1939–1951. [PubMed: 19288519]
40. Ix JH, et al. Fetuin-A and kidney function in persons with coronary artery disease--data from the Heart and Soul Study. Nephrol Dial Transplant. 2006; 21(8):2144–51. [PubMed: 16644775]
41. Ruhaak LR, et al. Hydrophilic interaction chromatography-based high-throughput sample preparation method for N-glycan analysis from total human plasma glycoproteins. Anal Chem. 2008; 80(15):6119–26. [PubMed: 18593198]
42. Schauer R. Sialic acids as regulators of molecular and cellular interactions. Current Opinion in Structural Biology. 2009; 19(5):507–514. [PubMed: 19699080]
43. Varki A. Sialic acids in human health and disease. Trends in Molecular Medicine. 2008; 14(8): 351–360. [PubMed: 18606570]
44. Zhuo Y, Chammas R, Bellis SL. Sialylation of β1 Integrins Blocks Cell Adhesion to Galectin-3 and Protects Cells against Galectin-3-induced Apoptosis. Journal of Biological Chemistry. 2008; 283(32):22177–22185. [PubMed: 18676377]
45. Kumari K, et al. Receptor binding specificity of recent human H3N2 influenza viruses. Virology Journal. 2007; 4(1):42. [PubMed: 17490484]
46. Neu U, et al. Structural basis of GM1 ganglioside recognition by simian virus 40. Proceedings of the National Academy of Sciences. 2008; 105(13):5219–5224.
47. Boucher JG, Nguyen T, Sparks DL. Lipoprotein electrostatic properties regulate hepatic lipase association and activity. Biochem Cell Biol. 2007; 85(6):696–708. [PubMed: 18059528]
48. Masson D, Athias A, Lagrost L. Evidence for electronegativity of plasma high density lipoprotein-3 as one major determinant of human cholesteryl ester transfer protein activity. J Lipid Res. 1996; 37(7):1579–90. [PubMed: 8827528]
49. Ghosh P, et al. Effects of chronic alcohol treatment on the synthesis, sialylation, and disposition of nascent apolipoprotein E by peritoneal macrophages of rats. The American Journal of Clinical Nutrition. 2000; 72(1):190–198. [PubMed: 10871579]
50. Wopereis S, et al. Apolipoprotein C-III isofocusing in the diagnosis of genetic defects in O-glycan biosynthesis. Clin Chem. 2003; 49(11):1839–45. [PubMed: 14578315]
51. Nwosu CC, et al. J. Proteome Res. 2011; 10(5):2612. [PubMed: 21469647]
52. Ix JH, et al. Fetuin-A and kidney function in persons with coronary artery disease—data from the heart and soul study. Nephrology Dialysis Transplantation. 2006; 21(8):2144–2151.
53. Ix JH, et al. The Associations of Fetuin-A With Subclinical Cardiovascular Disease in Community-Dwelling Persons: The Rancho Bernardo Study. Journal of the American College of Cardiology. 2011; 58(23):2372–2379. [PubMed: 22115642]
54. Ketteler M, et al. Association of low fetuin-A (AHSG) concentrations in serum with cardiovascular mortality in patients on dialysis: a cross-sectional study. The Lancet. 2003; 361(9360):827–833.
55. Jahnen-Dechent W, et al. Fetuin-A Regulation of Calcified Matrix Metabolism. Circulation Research. 2011; 108(12):1494–1509. [PubMed: 21659653]
56. Ketteler M, Schlieper G, Floege J. Calcification and Cardiovascular Health: New Insights Into an Old Phenomenon. Hypertension. 2006; 47(6):1027–1034. [PubMed: 16618842]
57. Zauner G, et al. Protein glycosylation analysis by HILIC-LC-MS of Proteinase K-generated N- and O-glycopeptides. Journal of Separation Science. 2010; 33(6-7):903–910. [PubMed: 20222081]
58. Corvol P, Jeunemaitre X. Molecular Genetics of Human Hypertension: Role of Angiotensinogen. Endocrine Reviews. 1997; 18(5):662–677. [PubMed: 9331547]
59. Gimenez-Roqueplo A-P, et al. Role of N-Glycosylation in Human Angiotensinogen. Journal of Biological Chemistry. 1998; 273(33):21232–21238. [PubMed: 9694881]
60. Ishioka N, Takahashi N, Putnam FW. Amino acid sequence of human plasma alpha 1B-glycoprotein: homology to the immunoglobulin supergene family. Proceedings of the National Academy of Sciences. 1986; 83(8):2363–2367.

61. Nelsestuen Gl Fau - Zhang, Y., et al. Plasma protein profiling: unique and stable features of individuals. (1615-9853 (Print))
62. Harvey SB, et al. O-Glycoside Biomarker of Apolipoprotein C3: Responsiveness to Obesity, Bariatric Surgery, and Therapy with Metformin, to Chronic or Severe Liver Disease and to Mortality in Severe Sepsis and Graft vs Host Disease. Journal of Proteome Research. 2008; 8(2): 603–612. [PubMed: 19055479]
63. von Eckardstein A, et al. Apolipoprotein C-III(Lys58----Glu). Identification of an apolipoprotein C-III variant in a family with hyperalphalipoproteinemia. The Journal of Clinical Investigation. 1991; 87(5):1724–1731. [PubMed: 2022742]
64. Riwanto M Fau - Rohrer, L., et al. Altered activation of endothelial anti- and proapoptotic pathways by high-density lipoprotein from patients with coronary artery disease: role of high-density lipoprotein-proteome remodeling. (1524-4539 (Electronic))
65. Mange A Fau - Goux, A., et al. HDL proteome in hemodialysis patients: a quantitative nanoflow liquid chromatography-tandem mass spectrometry approach. (1932-6203 (Electronic))
66. Lee H, et al. Multiple Precursor Ion Scanning of Gangliosides and Sulfatides with a Reversed-Phase Microfluidic Chip and Quadrupole Time-of-Flight Mass Spectrometry. Analytical Chemistry. 2012; 84(14):5905–5912. [PubMed: 22697387]
67. Senn H-J, et al. Gangliosides in normal human serum. European Journal of Biochemistry. 1989; 181(3):657–662. [PubMed: 2731542]
68. Prokazova NV, et al. The gangliosides of adult human aorta: intima, media and plaque. Eur J Biochem. 1987; 167(2):349–52. [PubMed: 3622519]
69. Mukhin DN, et al. Ganglioside content and composition of cells from normal and atherosclerotic human aorta. Atherosclerosis. 1989; 78(1):39–45. [PubMed: 2757685]
70. Bezuglov VV, et al. [Gangliosides modulate lipoxygenase oxidation in human lymphocytes]. Biokhimiia. 1991; 56(2):267–72. [PubMed: 1908320]
71. Garner AE, Smith DA, Hooper NM. Sphingomyelin chain length influences the distribution of GPI-anchored proteins in rafts in supported lipid bilayers. Mol Membr Biol. 2007; 24(3):233–42. [PubMed: 17520480]
72. Sorci-Thomas MG, et al. Nascent high density lipoproteins formed by ABCA1 resemble lipid rafts and are structurally organized by three apoA-I monomers. J Lipid Res. 2012; 53(9):1890–909. [PubMed: 22750655]

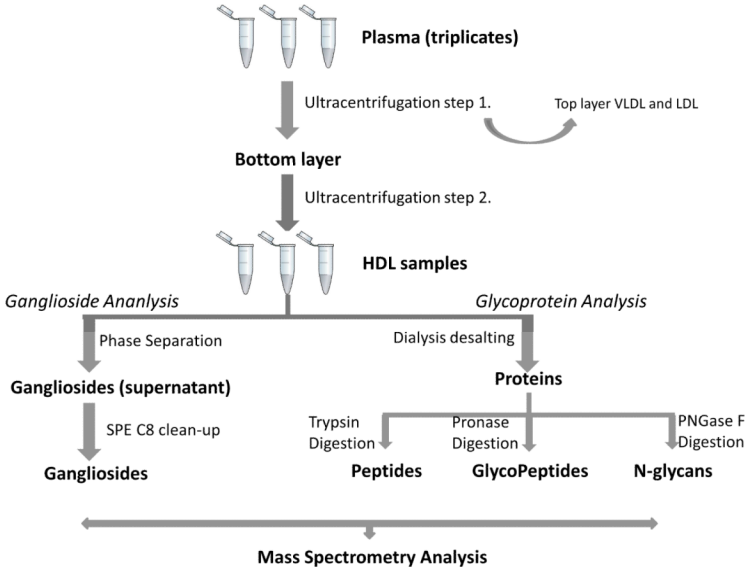

Figure 1.
HDL glycome analysis workflow.

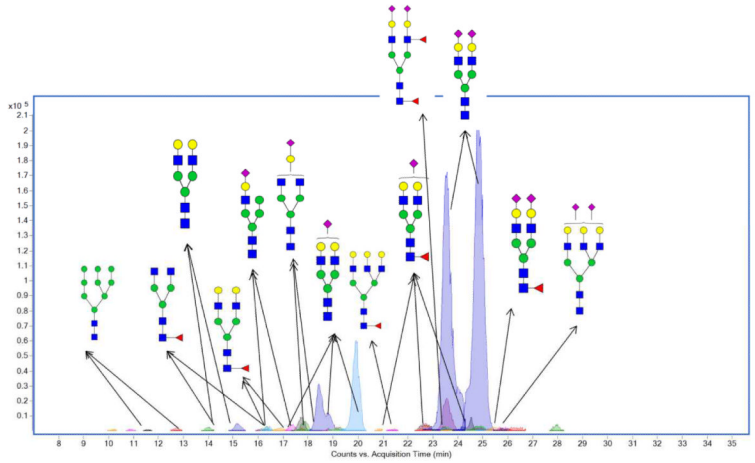

Figure 2.

Overlaid extracted compound chromatograms (ECCs) showing the profile of human HDL glycans via nano-LC/MS. Green circles, yellow circles, blue squares, red triangles, and purple diamonds represent mannose, galactose, GlcNAc, fucose, and NeuAc residues, respectively.

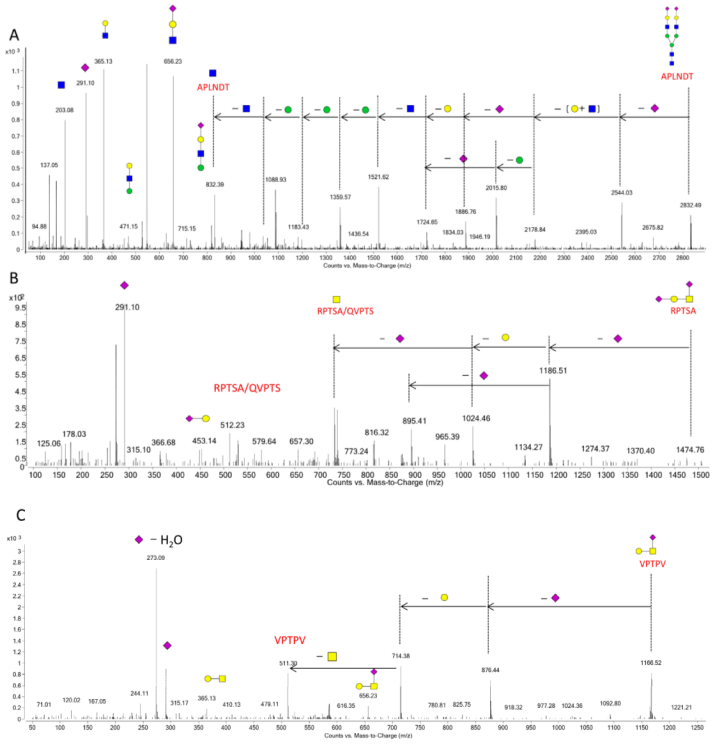

Figure 3.

Deconvoluted MS/MS spectra of three sialylated glycopeptides. (A) MS/MS data for an N-linked glycopeptide from fetuin A in HDL protein mixture; (B and C) MS/MS data for O-linked glycopeptides from Apolipoprotein C3 and fetuin A, respectively.

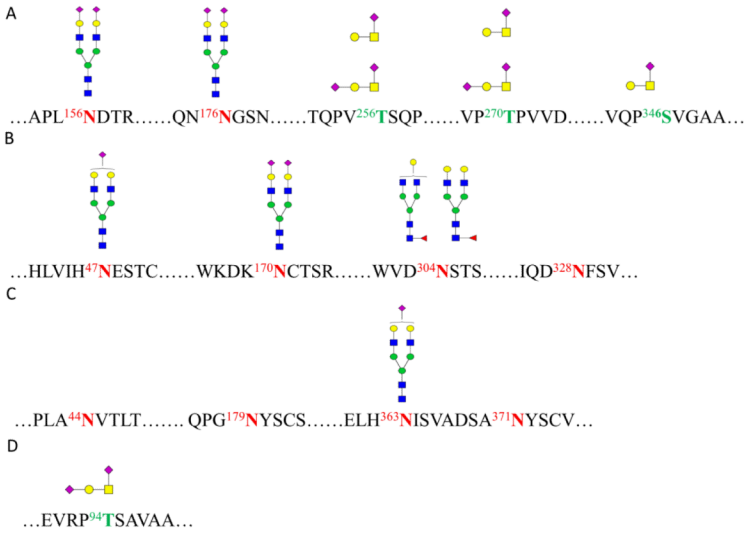

Figure 4.

Glycan site-heterogeneity of HDL associated glycoprotein A) Fetuin A (Alpha-2-HS-glycoprotein), B) Angiotensinogen, C) Alpha-1B-glycoprotein, and D) Apolipoprotein CIII.

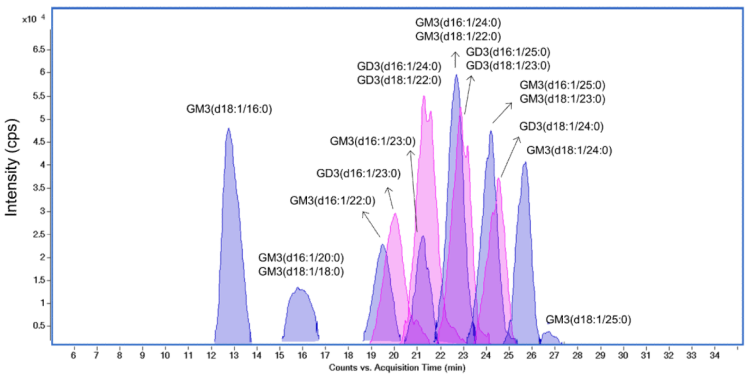

Figure 5.

Overlaid extracted compound chromatograms (ECCs) showing the profile of human HDL ganglioside via nano-LC/MS. Analysis of the accurately measured masses corresponding to each peak in chromatograms reveals monosialylated ganglioside (GM3, peaks shaded in blue) and disialylated ganglioside (GD3, peaks shaded in pink).

Table 1

List of HDL glycans with retention times, their m/z values, charge states, glycan compositions, and the ion intensities.

Retention time (min)	Measured m/z	Charge state	Mass error (ppm)	Hexose	HexNAc	Fucose	NeuAc	Ion Intensity (counts)
24.839	1112.403	2	3.57	5	4	0	2	6091078
23.541	1112.402	2	2.94	5	4	0	2	4906932
19.915	966.8551	2	4.13	5	4	0	1	1196125
18.466	966.8576	2	6.78	5	4	0	1	797081
22.675	966.8543	2	3.37	5	4	0	1	129647
17.355	966.8556	2	4.65	5	4	0	1	78041
17.725	865.3141	2	3.12	5	3	0	1	171480
16.31	865.3134	2	2.38	5	3	0	1	47271
24.524	1039.883	2	2.91	5	4	1	1	141126
22.706	1039.883	2	2.99	5	4	1	1	95666
23.434	1039.884	2	3.92	5	4	1	1	41850
20.862	1039.878	2	−1.68	5	4	1	1	19297
17.857	894.3368	2	4.97	5	4	1	0	140215
16.374	894.3332	2	0.98	5	4	1	0	58633
15.169	821.3112	2	9.56	5	4	0	0	93233
13.997	821.3069	2	4.31	5	4	0	0	43677
25.483	1185.427	2	−0.37	5	4	1	2	62932
19.253	784.2855	2	0.65	4	3	0	1	55095
16.874	813.3067	2	0.92	4	4	1	0	53118
19.206	885.8271	2	2.78	4	4	0	1	48338
17.746	885.8248	2	0.15	4	4	0	1	24690
12.726	942.3367	2	7.5	9	2	0	0	38575
11.579	942.3349	2	5.58	9	2	0	0	16327
23.563	1258.465	2	6.4	5	4	2	2	37927
21.401	1076.901	2	2.33	6	5	1	0	30048
24.534	1294.957	2	−5.19	6	5	0	2	25651
16.092	732.2802	2	0.95	3	4	1	0	22085

Table 2

List of glycopeptides from HDL glycoproteins with retention time, their m/z values, glycan composition, the protein, the sequence of the peptide, and the glycosylation site.

Retention Time (min)	Measured m/z	Charge state	Mass Error (ppm)	Hexose	HexNAc	Fucose	NeuAc	Protein	Sequence	site
24.893	967.7219	3	12.13	5	4	0	2	HEMO	LPQPQN	453
25.338	945.7015	3	1.61	5	4	0	2	FETUA	APLNDT	156
22.66	875.6656	3	11.12	5	4	0	2	TRFE	SNVT	630
21.539	865.9789	3	7.70	5	4	0	2	FETUA	NGSN	176
21.539	865.9789	3	7.70	5	4	0	2	APO-H	GNNS	163
21.205	856.3226	3	8.25	5	4	0	2	KNG1	QTN	205
21.205	856.3226	3	13.68	5	4	0	2	A1AT	GNAT	271
17.342	851.6635	3	14.67	5	4	0	2	FETUA	NKS	432
23.225	851.3275	3	5.01	5	4	0	2	A1AT	NLT	107
17.54	822.6527	3	9.53	5	4	0	2	ANGT	KN	170
15.447	697.2652	3	17.33	5	4	1	0	A1AT	NST	70
15.447	697.2652	3	19.91	5	4	1	0	ANGT	NST	304
14.503	643.2539	3	4.78	4	4	1	0	HEMO	NST	246
16.925	728.6016	3	19.26	5	4	0	1	ANGT	HN	47
13.771	594.2537	2	0.93	1	1	0	1	FETUA	VTSQP	256
13.957	594.2637	2	12.90	1	1	0	1	KNG1	KTEGP	542
14.090	572.243	2	6.96	1	1	0	1	FETUA	QPSVG	346
21.75	721.3209	2	8.46	1	1	0	1	HEMO	SLAIATPL	24
24.809	730.3203	2	6.19	1	1	0	2	FETUA	VPTPV	270
19.01	739.8152	2	14.86	1	1	0	2	FETUA	VTSQP	256
18.797	739.8152	2	1.976	1	1	0	2	APOCIII	RPTSA	94
18.717	584.7726	2	18.75	1	1	0	1	FETUA	VPTPV	270
26.005	830.3642	2	18.21	1	1	0	2	FETUA	EAVPTPV	270

Abbreviations: HEMO, hemopexin; FETUA, fetuin A; TRFE, serotransferrin; APO-H, apolipoprotein H; KNG1, kininogen-1; A1AT, alpha-1-antitrypsin; ANGT, Angiotensinogen; APOCIII, Apolipoprotein CIII

Table 3

List of HDL gangliosides with retention times, their m/z values, charge states, assignments, and the ion intensities.

Retention time (min)	Measured m/z	Charge state	Mass error (ppm)	Structural Assignment	Ion Intensity (counts)
12.9	1151.711	−1	−4.3	GM3(d18:1/16:0)	1120103
16.2	1179.732	−1	4.2	GM3(d16:1/20:0) or GM3 (d18:1/18:0)	498901
19.7	1207.760	−1	7.5	GM3(d16:1/22:0)	459570
21.4	1221.779	−1	4.1	GM3(d16:1/23:0)	288025
22.9	1235.793	−1	5.7	GM3(d16:1/24:0) or GM3(d18:1/22:0)	772085
24.3	1249.812	−1	2.4	GM3(d16:1/25:0) or GM3(d18:1/23:0)	543404
25.8	1263.833	−1	−1.6	GM3(d18:1/24:0)	494824
26.7	1277.849	−1	−1.6	GM3(d18:1/25:0)	42591
20.2	755.935	−2	1.3	GD3(d16:1/23:0)	455116
21.4	762.945	−2	−1.3	GD3(d16:1/24:0) or GD3(d18:1/22:0)	1006020
23.1	769.972	−2	1.3	GD3(d16:1/25:0) or GD3(d18:1/23:0)	815475
24.7	776.960	−2	0.0	GD3(d18:1/24:0)	523004